

Diode parameters design simulation and experimental validation against silver migration phenomena in high voltage switching application

Mattia Gianfranco Gentile, Physics Department, University of Torino, Turin, Italy, mattia1gentile@gmail.com

Luigi Merlin, Vishay Semiconductor Italiana S.p.A., Italy, luigi.merlin@vishay.com.

Paolo Mirone, Department of Information Technology and Electrical Engineering (DIETI), University Federico II, Naples, Italy, paolomirone@gmail.com

Ettore Vittone, Physics Department, University of Torino, Turin, Italy, etto.vittone@unito.it

Abstract

Metallic Electro Chemical Migration (ECM) is a phenomenon has long been recognized as a significant failure pathway of electronic devices. In this work, silver ECM was investigated and analyzed in commercial silicon power diodes.

Dedicated test procedures have been performed in order to study the Ag ECM triggering and evolution. 2D TCAD simulations were used to analyze the ECM phenomena at the diode edge termination, identifying design solutions able to mitigate such effect. Finally, the proposed device has been experimentally validated and results highlight a significant reduction of devices failure.

1. INTRODUCTION

Soldering is one of the key technologies for assembling microelectronic component [1][2][3]. Recently surface mount technology has become the primary process to produce high functional, high response compact and light weight electronic products [4]. Also the size of the component and conductor spacing has been reduced. A board with a high density of components generates much more heat during operation resulting in more severe thermal fatigue of soldered joints [5]. Various metallization type are applied in advanced high-density interconnection systems. The integration of these metallization processes is determined, not only by technological factors, but also by those physical and chemical processes that could cause short circuit formation [5].

ECM has long been recognized as a significant potential failure mode in many electrical and electronic systems [1] [6] [7] [8] [9] [10] [11].

The ECM is a well-known mechanism, under the

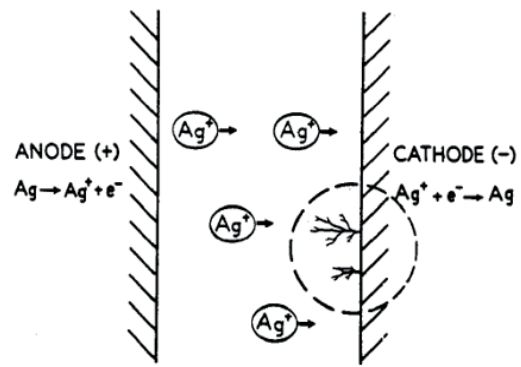


Fig.1: Schematic diagram of early stages of dendrite growth (adapted from [1]).

influence of an applied electric field, divided in three steps (Fig. 1): metal dissolution at anode, metal ions transportation along the moisture path and deposition of metal ions, as pure metal, on the cathode [1] [6] [12] [13].

The metal migration is recognizable like a sort of dendritic and filament structures with a wide variety of shapes (Fig. 2) [14]. The morphology differences between the dendritic structures could be related to the magnitude of the electric field, the metal composition, impurities, substrate, water film absorbed and pH distribution [15].

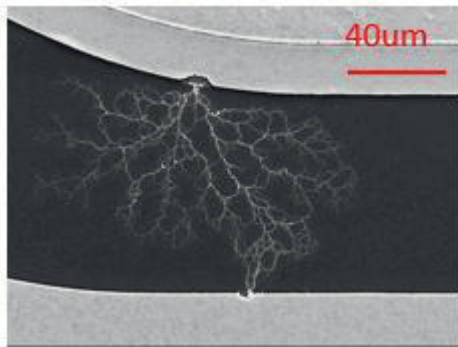


Fig.2: Examples of silver filament.

These filaments bring the formation of metallic bridges between two adjacent electrodes; these conductive pathways induce leakage failure or short-circuit in the devices [6].

The humid ECM is promoted by moisture [16], contaminations on the insulator surface [17], voltage difference between conductors, narrow spacing widths, elevated temperatures [1] [18] [19] [20] [21].

The migration ability of metallization systems is correlated with the solubility products of metal hydroxide. The ECM ranking can be defined as follows: $Ag > Pb > Cu > Sn$ [5].

In particular, the Ag, with an anodic dissolution rate that can reach $10^{-1} A/cm^2$, which corresponds to a catastrophic removal rate of 35.6 nm/s [12], is very susceptible to ECM phenomena.

This contribution is focused on humid ECM, which appear as metallic dendrites resulting in electrical failures of microelectronic devices. In particular, the ECM failure mode has been analyzed on diodes in four different designs. The design parameters, modified in the tested samples, were: the protection of the insulator from the moisture, obtained with the presence of a Passivation Layer (PL) and a new reshape of the termination part of Ag layer able to prevent the formation of an electric field peak on the silver layer. TCAD simulations [22] show the beneficial effect introduced by the new design solution, resulting in a movement of the maximum electric field peak from the Ag layer to a different metal layer, less susceptible to ECM phenomena [5].

The samples were employed in a typical application for 168 hr. After the use, the presence of silver trees has been evaluated and correlated with a characteristic parameter, i.e. the leakage current (I_r) [23], which is a commonly used as reference parameter to identify the devices degradation.

2. EXPERIMENTAL DETAILS

2.1. Tested devices

The tested devices are commercial p-n junction diodes 200V rated with Ag electrodes. Fig. 3 shows the schematic cross section of the device.

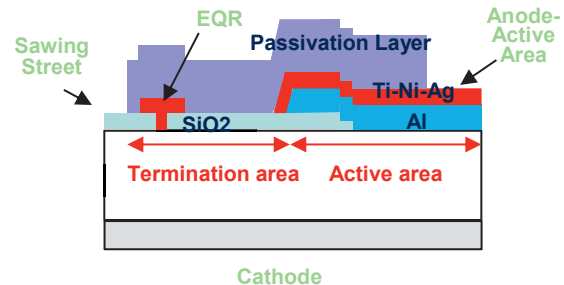


Fig.3: Schematic cross section view of the device termination under study.

The structure composed by an Active Area (AA) and a termination area [24]. At the end of termination there is an Equal Potential Ring contact (EQR), connected to the n-substrate. In forward condition, the anode potential is positive with respect to the cathode potential and therefore with respect to the EQR. On contrary, in reverse blocking, the cathode potential is higher than the anode one.

The metal layer consists of four layers: aluminum (Al) top covered by titanium (Ti), nickel (Ni) and silver (Ag) for the anode contact and Ti, Ni and Ag for the EQR. The ratio between layers thickness is 15Al:1Ti:1Ni:5Ag.

The metal process has been divided in two main steps:

- Al deposition, mask and etch metal process.
- Ti, Ni, Ag deposition, mask and etch metal process.

The etch solutions were chosen for their selectivity in the metal etching [25]. The wet etch isotropic nature [25] generates an under etching of the metal and creates a sort of “roof” in the metal layer (Fig.4).

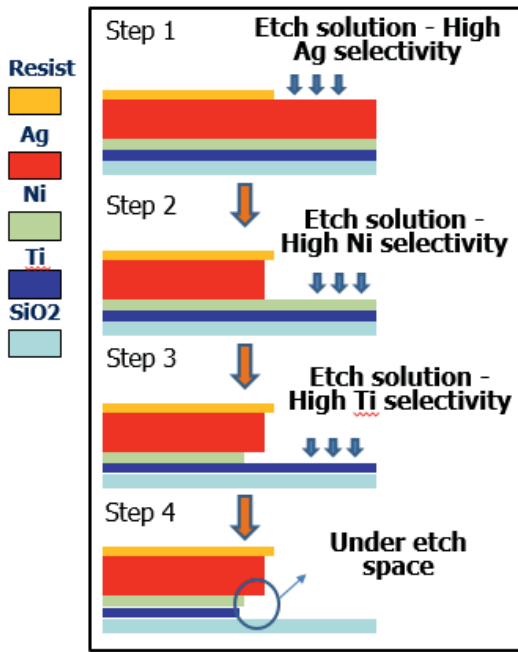


Fig.4: Tri-metal process etching divided step by step. Step 1: Ag etch with $\text{NH}_4\text{OH}:\text{H}_2\text{O}_2:\text{H}_2\text{O}$ solution, step 2: Ni etch with $\text{HNO}_3:\text{H}_2\text{O}$ solution, step 3: Ti etch with $\text{HF}:\text{H}_2\text{O}$ solution. The presence of the metal “roof” depends of the isotropic nature of the wet etch.

The Ag roof on the SiO_2 , is achieved with a Standard Metal Process (SMP) etch, creating a region, in which the moisture can be trapped. By using a different mask design, the Ag roof has been eliminated (Fig. 5).

The resulting new structure is called Pull-Back design (PB).

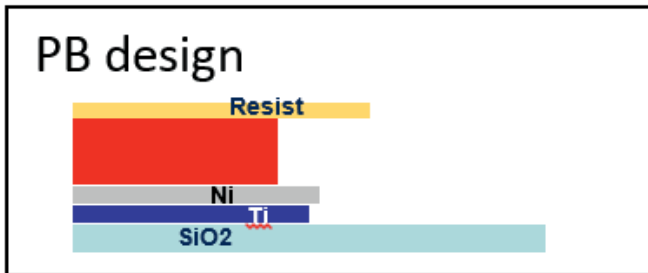


Fig.5: the Pull Back mask design eliminated the “Ag metal roof”.

In the new tests Ag layer has been modified on the edge and with the two different option proposed a PL has been added. Four different designs were studied (Fig. 6).

Standard metal process (SMP) is the design that shows a sort of Ag roof that creates a region, where moisture can be trapped. With the PB design the Ag roof it was removed.

The effect of a PL has been considered with the structure: SMP+PL and PB+PL respectively (Fig.6).

Standard Metal Process (SMP)		
Pull Back Process (PB)		
SMP + Passivation Layer (PL)		
Pull Back Process + Passivation Layer		

Fig.6: Schematic cross section views and SEM pictures of the four design in exam. SMP standard metal process, PB pull back process, SMP+PL standard metal process with passivation layer, PB+PL pull back process with passivation layer.

Finally, the devices have been assembled with standard Surface Mount Packages (SMP).

2.2. Test equipment

The adopted test accelerates the degradation condition that the device would have during its whole lifetime. The test consists on positioning the devices in a pressure cooking temperature (PCT) for 24 hours, at 121 °C, humidity 100%. In order to saturate the devices and the packages with moisture and simulate an environment with high humidity concentration. Afterwards the devices have been tested in a commercial set-up with a fly-back circuit for 168hr. The driver circuit switches at 50 kHz, working in forward and reverse polarization, in a range of 180-200 V with a forward current of 2 A.

At the end of the test, each device has been electrically characterized by a standard probe system, measuring the leakage (I_r) value.

In order to carry out the morphological analysis to verify the presence of silver bridges between AA and EQR, the package was removed by using H_2SO_4 etching. The microscopic analysis were carried out with a ZEISS Auriga dual beam-field emission scanning electron microscope (Field Emission Scanning Electron Microscopy (FESEM)).

3. TCAD SIMULATIONS.

ECM phenomenon can be associated to different physical causes, including the presence of a high Electric Field (EF). Such phenomenon was analyzed in detail by means of 2D TCAD simulations. The structure of Fig.3 was appropriately realized using the suite of tools Sentaurus simulating a real operative condition for the devices.

Simulations have been led by considering the whole edge termination structure of Fig.3. During the turn-off condition, the device is in reverse polarization and the voltage drop between the two contacts can led the generation of a high EF in the structure. Fig.7 and Fig.8 show the EF distribution of the analyzed structure; during the reverse polarization highlighting the presence of the high electric field in both device structures SMP and PB. It is pointed out as the EF, for the former, directly occurs at the edge of the metallic Ag plate while the PB solution considerably reduces its effect on the Ag metal.

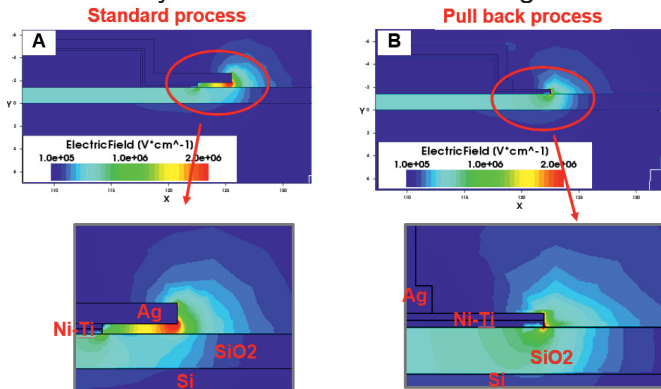


Fig.7: TCAD simulation in reverse voltage. A) Electric field distribution in SMP Ag shape layer, B) electric field distribution in PB Ag shape layer.

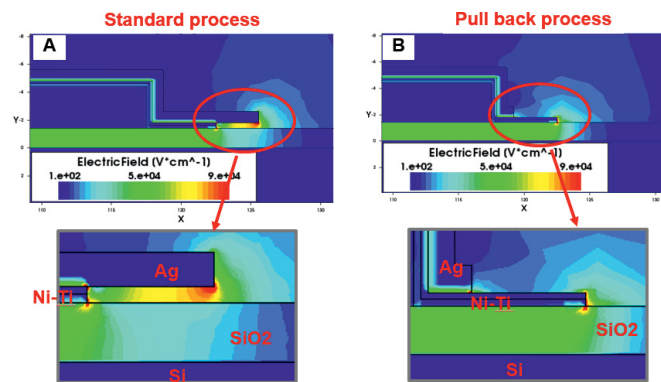


Fig.8: TCAD simulation in forward voltage. A) Electric field distribution in SMP Ag shape layer, B) electric field distribution in PB Ag shape layer.

The Ag roof (Fig.7A and Fig.8A) generated by the etching, can lead to void areas interposed between Ag plate and silicon dioxide. In this condition, a high EF is generated into the air zone due to the lower dielectric constant of this last. It can be explained by applying the Gauss's law to the interface layers:

$$E_{air}\epsilon_{air} = E_{Ox}\epsilon_{Ox} = E_{Si}\epsilon_{Si}$$

where E_x and ϵ_x are the EF and dielectric constant of material X, respectively.

Since the $\epsilon_{Air} \approx 1$, $\epsilon_{Ox} \approx 3.9$, $\epsilon_{Si} \approx 11.9$, it turns out that E_{Air} is about 4 times higher than in the oxide layer and 12 time higher than in silicon. This situation (Fig.9) might lead to the electrostatic discharge generation due to the low air dielectric rigidity (3 kV/mm). Under the EF effect at the Ag surface, ions can move from the cathode to the anode promoting the ECM phenomenon.

Appropriate design solution has been introduced in order to reduce the possibility of ions migration. It consists of reducing the Ag layer width and extending the Ni-Ti layer beyond, taking away any possibilities to generate vacuum zones during the chemical etching. In this way the high EF was kept distant from the Ag surface by reducing the portion of Ag that overlaps the Ni-Ti layer (see Fig.7B and Fig.8B).



Fig.9: Dielectric stack between metal and silicon.

4. RESULTS

For each group the same amount of devices have been tested, all samples failed in the electrical test and Fig. 10 shows the typical appearance of the failed devices.

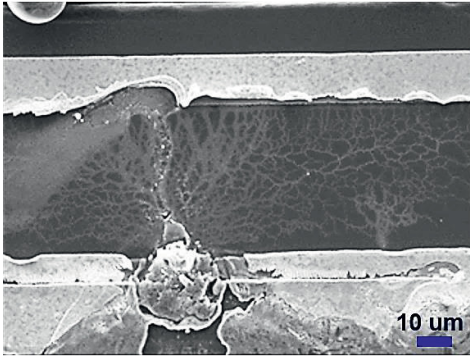


Fig.10: Failed device show the typical ECM "tree". It creates a conductive path and bring short circuit.

The failure rates relevant to the four analyzed designs are shown in Fig.11. In particular, the different failure behaviors are analyzed with the presence of the PB design and the PL. With the SMP, the failed devices were a certain amount (X), adding the PL on the devices termination the devices failed were reduced at X/3. The PB process without PL have showed a failure rate of X/5, with the PB process and the PL no devices showed leakage fail after the test.

In order to determine significant differences between the expected frequencies and the observed frequencies, the statistical test chi-squared has been used, the statistical significance between the population groups with a probability level of 5% has been assumed. These results show as in presence of PL and the PB solutions the device failure rate is considerably reduced.

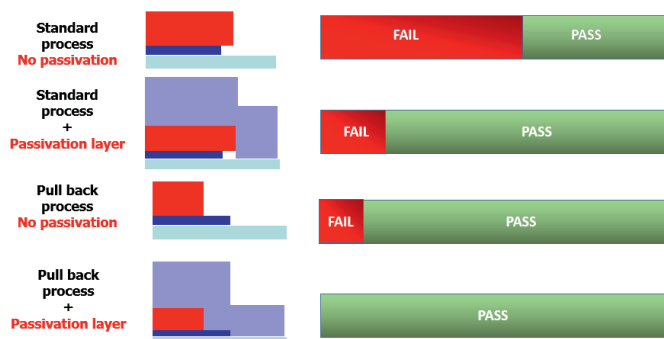


Fig.11: Failure rate for different designs in study.

5. CONCLUSION

The ECM has long been a significant potential failure mode in many electrical and electronic systems, recognizable like a sort of dendritic and filament structure with a wide variety of shape. These filaments bring the formation of metallic bridges between two adjacent electrodes; these conductive pathways induce leakage failure or short-circuit in the devices

The ECM is a well-known mechanism, under the influence of an applied electric field, divided in three steps: metal dissolution at anode, metal ions transportation along the moisture path and deposition of metal ions, as pure metal, on the cathode.

Many different parameter work for the promotion of humid ECM in particular:

- Moisture creates a low resistance electrolytic path
- Contamination on the insulator increases the adsorption of water, the conductivity and the silver dissolution
- Electric field is the major driver in moving Ag⁺ ions
- Elevated temperature increases the conductivity of the electrolytic surface

The literature reports different possibility for a good ECM prevention but not all are applicable on real commercial devices, in particular when it is request a complex material and geometry change. In this work, a test system has been developed to test commercial devices and many tests; it reaches a significant mitigation of ECM phenomena. The best design conditions have been achieved combining the presence of a passivation layer, to protect the device from the moisture, and reducing the portion of Ag in the termination.

The chemical etch process generates void zone adjacent to Ag metal. The 2D TCAD simulation showed as the presence of the Ag roof in the termination design presents a high EF generated in a void zone adjacent to Ag metal due to the lower dielectric constant.

To reduce the possibility of ions migration, it has been removed void zone with a pull-back process. Furthermore, the high EF was kept distant from the Ag surface by reducing the portion of Ag that overlaps the Ni-Ti layer.

6. REFERENCES

- [1] J. Krumbein, *33 rd meeting of the IEEE holm conference*, 1987. DOI 10.1109/ TCHMT.1988. 1134880
- [2] Charles Harper, *Electronic Materials and Processes Handbook*, McGraw-Hill Professional, 2003 ISBN-13: 978-0071402149
- [3] M. Gentile, J. Muñoz-Tabares, L. Merlin and E. Vittone, "Marbled Texture of sputtered Al/Si alloy thin film on Si," *Thin solid film*, vol. 612, p. 165, 2016.
- [4] T. Takemoto, R. Latanision, T. W. Eagar and A. Matsunawa, "Electrochemical migration tests of solder alloys in pure water," *Corrosion Science*, pp. 1415-1430, 1997.
- [5] G. Harsanyi and G. Inzelt, comparing migratory resistive short formation abilities of conduct systems applied in advanced interconnection systems, *Microelectronic reliability*, vol. 41, pp. 229-237, 2001. DOI 10.1016/S0026-2714(00)00093-7.
- [6] J. Krumbein, "Tutorial: electrolytic models for metallic electromigration failure mechanisms," *IEEE transaction on reliability*, vol. 44, pp. 539-549, 1995.
- [7] R. Shields, "Some characteristics of metal migration in or on the surface insulators," in *Atomic energy of Canada limited*, Ontario, 1979.
- [8] R. Johnson, "Construction of filament surfaces," *Phys Rev*, vol. 54, p. 459, 1938.
- [9] R. Koo, "Observation on Electromigration and improved filament life of microminiature lamps," *Illum. Eng. Soc.*, vol. 4, pp. 19-24, 1974.
- [10] J. Peacock and A. Wilson, "Electrotransport of tungsten and life of a pilament," *Appl.Phys*, vol. 13, p. 6037, 1968.
- [11] I. Blench, "A study of failure mechanisms in silicon planar epitaxial transistor," 1965.
- [12] K. Vu, "Silver migration - The mechanism and effects on thick-film conductors," *Material science engineering*, 2003.
- [13] S. Krumbein, *IEEE transaction on reliability*, vol. 44, pp. 539-549, 1995. DOI 10.1109/24.475971
- [14] C. Gabrielli, L. Beitone, C. Mace, E. Ostermann and H. Perrot, "Electrochemistry on microcircuits. II: Copper dendrites in oxalic acid," *Microelectronic Engineering*, vol. 85, no. doi: 10.1016, p. 1686–1698, 2008.
- [15] M. Rosso, E. Chassaing, V. Fleury and J. Chazalviel, "Shape evolution of metals electrodeposited from binary electrolytes," *Electroanalytical Chemistry*, vol. 559, pp. 165-173, 2003.
- [16] B. Yan, S. Meilink, G. Warren and P. Wynblatt, "Water Adsorption and Surface Conductivity Measurements on a-Alumina Substrates," *IEEE TRANSACTIONS ON COMPONENTS*, vol. 2, pp. 247-251, 1987.
- [17] G. Harsanyi, "Irregular effect of chloride impurities on migration failure reliability: contradictions or understandable?," *Microelectronics Reliability*, vol. 39, pp. 1407-1411, 1999.
- [18] M. Reid, J. Punch, B. Rodgersa, M. J. Pomeroyb, T. Galkin, T. Stenberg, O. Rusanen, E. Elonen, M. Vilen and K. Viikevainen, "Factors that influence ionic migration on printed wiring boarding," *IEEE 43° Annual International Reliability Physics Symposium*, 2005.
- [19] B. Noh and S. Jung, "Characteristics of environmental factor for electrochemical migration on printed circuit board," *J Mater Sci*, vol. 19, no. DOI 10.1007/s10854-007-9421-3, p. 952–956, 2008.
- [20] J. Lin and J. Chan, "On the resistance of silver migration in Ag-Pd conductive thick films under humid environment and applied d.c. field," *Materials Chemistry and Physics*, vol. 43, pp. 256-265, 1996.
- [21] G. DiGiacomo, "Metal migration (Ag, Cu, Pb) in encapsulated modules and time to fail model as a function of the enviroment and package properties".
- [22] Sentaurus TCAD, *Synopsys Inc.*, K-2015.06
- [23] C.T. Sah, R.N. Noyce, and W. Shockley, "Carrier Generation and Recombination in P–N Junctions and P–N Junction Characteristics," *Proceedings of the IRE*, Vol. 45, pp. 1228–1243, 1957.
- [24] B. Jayant Baliga. *Fundamentals of power semiconductor devices*. Springer Science & Business Media, 2010.
- [25] Karena A. Reinhardt, Werner Kern, "Silicon wafer cleaning technology", William Andrew, USA, 2007.